



Cite this: *Org. Biomol. Chem.*, 2017, **15**, 5161

Isonucleotide incorporation into middle and terminal siRNA duplexes exhibits high gene silencing efficacy and nuclease resistance†

Yuan Ma,^{‡a} Shuang Liu,^{‡a} Yusi Wang,^a Yuanhe Zhao,^a Ye Huang,^a Lijun Zhong,^b Zhu Guan,^a Lihe Zhang^a and Zhenjun Yang^{ID} *^a

In this study, we introduced a pair of nucleotide enantiomers, D-/L-isonucleotides (D-/L-isoNA), to examine the interactions between siRNAs and their related proteins. The serum stability and gene-silencing activity of the modified siRNAs were systematically evaluated. Gene-silencing activity had a site-specific effect, and the incorporation of a single D-isoNA at the 8th position (counting from the 5'-terminus) in the antisense strand improved the gene-silencing activity by improving RISC loading and affecting the movement of the PIWI domain. D-isoNA incorporated at the terminus of siRNA including the 2nd position in the antisense strand and 3'-overhangs in the sense strand, especially the latter, enhanced nuclease resistance and prolonged the silencing retention time. In addition, L-isoNA incorporation into the middle of the sense strand enhanced activity. These results provide a chemical strategy for the modulation of siRNA gene-silencing activity and nuclease resistance.

Received 2nd May 2017,

Accepted 25th May 2017

DOI: 10.1039/c7ob01065f

rsc.li/obc

Introduction

RNA interference (RNAi), which is a natural process for regulating gene activities, has been regarded as a powerful tool for depressing gene expression. The RNAi approach was confirmed by double-stranded RNAs (dsRNAs) in *Caenorhabditis elegans* in 1998.¹ Small interfering RNAs (siRNAs) can be incorporated into the RNA-induced silencing complex (RISC), in which the antisense strand binds to the complementary mRNA by base-pairing and triggers its cleavage.² siRNAs are potential candidates for clinical application because they can be tailored to many disease-causing genes with high efficiency and specificity.³ However, there are some inherent limitations of oligonucleotides that must be overcome, such as susceptibility to cleavage by ribonucleases in serum,⁴ off-target effects,⁵ and the possibility of causing immune responses.⁶ Appropriate chemical modification is a considerable approach to optimize the biological and pharmacokinetic properties of siRNAs.⁷ Large conformational alterations are not tolerated, but minor

conformational alterations may improve the overall gene-silencing activities.⁸

Modified positions play a vital role in the biological efficiency of siRNAs. For example, phosphorylation of the first nucleotide in the 5'-terminus (the 1st position) is essential for silencing activity, which is usually intolerant to modifications, such as a locked nucleic acid (LNA).⁹ In addition, the seed region (the 2nd–8th positions) of siRNAs builds an A-form helix with the target mRNA,¹⁰ and significantly affects the guide-target base pairing in RISC.¹¹ Recently, Ian J. MacRae *et al.* analyzed the structures of Ago2 protein binding to a modified siRNA guide strand. They showed that the central seed sites (the 5th and 6th positions), which were modified with 2'-O-methyl (2'-O-Me) and 2'-fluoro (2'-F), deviated from the natural nucleotides in the modified complex.¹² Furthermore, the central region (the 9th–12th positions) is proximal to the cleavage sites. The modifications stabilizing the A-form and the minor groove may enhance the activity of 2'-O-Me, 2'-F and 8-oxoguanine (8-OG).¹³ In addition, the 3'-half region (the 13th–18th positions) assists in forming the hybridization duplex and improves the affinity to target mRNA,¹⁴ and enhancement of stability is obtained by utilizing 2'-O-Me.⁸ Moreover, the 3'-tail region (the 19th–21st positions) interacts with the PAZ domain of the Ago2 protein and protects siRNA from ribonuclease degradation.¹⁵ This conformational requirement is essential for siRNAs to interact properly with other proteins and their targets. For example, the A-form conformation of siRNAs is necessary for the stabilization of the Ago

^aState Key Laboratory of Natural and Biomimetic Drugs, School of Pharmaceutical Sciences, Peking University, Beijing, 100191, China. E-mail: yangzj@bjmu.edu.cn

^bMedical and Health Analysis Center, School of Pharmaceutical Sciences,

Peking University, No. 38 Xueyuan Road, Haidian District, Beijing 100191, China

†Electronic supplementary information (ESI) available. See DOI: 10.1039/c7ob01065f

‡These authors contributed equally to this paper.

protein.¹⁶ Furthermore, the secondary/tertiary structures of mRNAs influence the accessibility of RISC by hybridizing to the target.¹⁷

Although there have been many reports on chemical molecules incorporation into the siRNA duplex, several modifications successfully lead to optimization of its characteristics. However, analogs causing conformational alterations usually have diverse structures in comparison with natural nucleotides. For example, the 2'-O-MOE and LNA modifications show steric effects; however, the UNA modification shows molecular flexibility. Though the modifications lead to conformational distortion, the structures of these molecules are very different from those of natural nucleotides. An isonucleotide (isoNA) is a type of nucleotide analog, whose nucleobase is linked to a ribose at a position other than C-1', usually at C-2'.¹⁸ Isonucleotides can be divided into *D* and *L* configurations (Fig. 1), which show varying degrees of conformational alteration around the incorporation sites. Generally, *D*-isoNA incorporation leads to a minor rotational distortion to shorten the distance with the corresponding nucleotide in the siRNA. However, its enantiomer *L*-isoNA must rotate completely to fulfill base pairing, which consequently drastically affects the local conformation. The characteristic differences of *D*/*L*-isoNAs minimize except for conformational alteration. Through comparing the distinction of siRNAs respectively modified with *D*-isoNA and *L*-isoNA, we could clearly demonstrate how these alterations function in the RNAi approach. Therefore, isonucleotide modification could be used as a molecular tool to probe conformational requirement between nucleic acids and interactional biomacromolecules.

Previous reports have shown that siRNA modified with isoNAs at a specific position is likely to improve stability and activity.¹⁹ Nevertheless, we lack knowledge regarding the impact and molecular mechanisms of *D*/*L*-isoNAs' incorporation into various regions of siRNAs, such as the middle and terminus of the siRNA duplexes. To examine the effect of conformational distortion resulting from isoNA modification, we evaluated the biological properties, and moderate *D*/*L*-isoNAs were incorporated at the A-U sites in the siMB3 sequence, targeting the mutant BRAF-V600E.²⁰ Since *D*/*L*-isoNA incorporation might lead to a preferable conformational requirement, which is beneficial to the associated protein's recognition and

binding process, we assumed that an isoNA substitution at the proper position in siRNA would enhance its silencing activity and nuclease resistance.

Results

BRAF is a member of the Raf kinase family and is a member of the EGFR signaling pathway,²¹ which affects cell division, differentiation, and secretion. In the BRAF-V600E mutation, thymine is substituted with adenine at nucleotide 1799, which leads to valine (V) being substituted by glutamate (E) at codon 600. The frequency of the BRAF-V600E mutation varies widely in human cancers. In melanomas, more than 70% of the BRAF mutations are the V600E mutation, which makes it a potential drug target.²² RNase A is responsible for the degradation of siRNAs in the serum.²³ The A-U sites and the end of the siRNA duplex were identified as positions vulnerable to ribonucleases.²⁴ Additionally, there is a rigid nucleotide selectivity loop in the hAgo2 mid domain selecting for U and A monophosphates more actively than other nucleotide monophosphates.²⁵ Thus, we synthesized a series of *D*/*L*-isoNA modified siMB3s targeting the mutant Braf mRNA (BRAF V600E) (Table 1), and the modification was focused around the A-U sites to improve the biological properties that were involved in serum stability and

Table 1 Sequences of *D*/*L*-isoNA modified siMB3s

| | | | |
|---|--|-------------|--|
| Unmodified | 1 | siMB3 (S/A) | S: 5'-GCUACAGAGAAAUCUCGAUtt-3' A: 5'-AUCGAGAUUUCUCUGUAGCtt-3' |
| Sense strand modification (matched with siMB3-As) | 2 | S03D/A | 5'-GCU _D ACAGAGAAAUCUCGAUtt-3'/A |
| | 3 | S03L/A | 5'-GCU _L ACAGAGAAAUCUCGAUtt-3'/A |
| | 4 | S04D/A | 5'-GCUA _D CAGAGAAAUCUCGAUtt-3'/A |
| | 5 | S04L/A | 5'-GCUA _L CAGAGAAAUCUCGAUtt-3'/A |
| | 6 | S10D/A | 5'-GCUACAGAGA _D AAUCUCGAUtt-3'/A |
| | 7 | S10L/A | 5'-GCUACAGAGA _L AAUCUCGAUtt-3'/A |
| | 8 | S11D/A | 5'-GCUACAGAGA _D AUCUCGAUtt-3'/A |
| | 9 | S11L/A | 5'-GCUACAGAGA _L AUCUCGAUtt-3'/A |
| | 10 | S12D/A | 5'-GCUACAGAGAA _D UCUCGAUtt-3'/A |
| | 11 | S12L/A | 5'-GCUACAGAGAA _L UCUCGAUtt-3'/A |
| | 12 | S13D/A | 5'-GCUACAGAGAAA _D UCUCGAUtt-3'/A |
| | 13 | S13L/A | 5'-GCUACAGAGAAA _L UCUCGAUtt-3'/A |
| | 14 | S18D/A | 5'-GCUACAGAGAAAUCUCGA _D Utt-3'/A |
| | 15 | S18L/A | 5'-GCUACAGAGAAAUCUCGA _L Utt-3'/A |
| | Antisense strand modification (matched with siMB3-S) | 16 | S/A02D |
| 17 | | S/A02L | S/5'-AU _L CGAGAUUUCUCUGUAGCtt-3' |
| 18 | | S/A07D | S/5'-AUCGAG _D UUUCUCUGUAGCtt-3' |
| 19 | | S/A07L | S/5'-AUCGAG _L UUUCUCUGUAGCtt-3' |
| 20 | | S/A08D | S/5'-AUCGAGAU _D UUCUCUGUAGCtt-3' |
| 21 | | S/A08L | S/5'-AUCGAGAU _L UUCUCUGUAGCtt-3' |
| 22 | | S/A09D | S/5'-AUCGAGAU _D UCUCUGUAGCtt-3' |
| 23 | | S/A09L | S/5'-AUCGAGAU _L UCUCUGUAGCtt-3' |
| 24 | | S/A10D | S/5'-AUCGAGAUU _D CUCUGUAGCtt-3' |
| 25 | | S/A10L | S/5'-AUCGAGAUU _L CUCUGUAGCtt-3' |
| 26 | | S/A16D | S/5'-AUCGAGAUUUCUCUGU _D AGCtt-3' |
| 27 | | S/A16L | S/5'-AUCGAGAUUUCUCUGU _L AGCtt-3' |
| 28 | | S/A17D | S/5'-AUCGAGAUUUCUCUGU _D GCtt-3' |
| 29 | | S/A17L | S/5'-AUCGAGAUUUCUCUGU _L GCtt-3' |

The positions of *D*/*L*-isoNA incorporation are indicated in blue italic and bold. "B_D" represents *D*-isoNA modification; "B_L" represents *L*-isoNA modification.

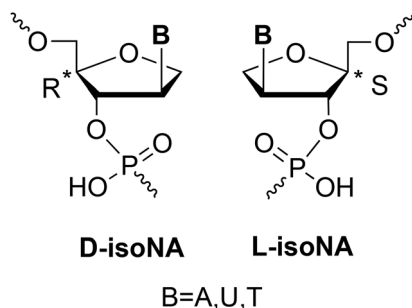


Fig. 1 The structure of *D*/*L*-isoNAs.

silencing activity. All of the sequence details of the synthesized oligonucleotide strands are shown in Table S1.†

Antisense strand of siRNAs modified with D-/L-isoNAs

The serum stabilities of siMB3s modified with D-/L-isoNA were analyzed (Fig. 2A and B), and siQuant assays were also performed to evaluate their gene-silencing activities (Fig. 2C). In brief, a short target sequence complementary to the siRNA antisense strand was fused in frame with the firefly luciferase gene in a eukaryotic expression vector. The resulting fusion reporter was transfected into cultured HEK293 cells, together with siRNA and a *Renilla* luciferase normalization vector. The relative luciferase levels were inversely proportional to the gene-silencing activities of siRNA.

In our case, we found that D-/L-isoNA incorporation in siMB3s exerted a different serum stability even at the same position. Natural siRNA (S/A) was significantly degraded within 3 h. siRNA with D-isoNA modified at the 2nd position (S/A02D) clearly exhibited initial bands after 12 h, though the silencing activity was slightly reduced. In addition, the activity of D-isoNA incorporation in the siMB3s tended to be site-specific, whereas the serum stability showed little change except at the 2nd position. The 9th position (S/A09D) and 16th position (S/A16D) modifications noticeably reduced activity. However, L-isoNA incorporation in the 3'-region of the antisense strand (S/A17L) significantly reduced serum stability. Furthermore, most siRNAs with L-isoNA incorporated in the antisense strand lost their activity. The activities of these siRNAs exhibited a significant difference on the unmodified sequence ($P < 0.0001$).

Only the S/A08D sequence exhibited a significant effect with activity enhancement in the siQuant assays. Though S/A07D and S/A10D seemed to lead to an enhancement of

activity, this result was not convincing enough to draw any conclusion. Thus, we further evaluated the activity of S/A08D in a western blot assay (Fig. 2D) and a real-time PCR assay (Fig. S1†). The results were consistent with the siQuant assay. This demonstrated that the 8th position was a precise site for D-isoNA modification in the antisense strand, which met the structural requirement of interactional regions by a slight conformational alteration. The activity of the sense strand was detected as well to estimate the off-target effect. siMB3 showed excellent target specificity at 5–30 nM (Fig. 2E). In addition, the D-/L-isoNA modifications did not influence the strand selection at the 8th position of the antisense strand (Fig. 2F).

Molecular mechanism for silencing enhancement of the 8th position modified with D-isoNA

To investigate whether the silencing enhancement is sequence-independent, we synthesized various siRNAs containing modified D-isoNA at the 8th position (Table 2). Due to the excellent strand selection of the siMB3 sequence, these novel siRNAs had inconspicuous terminal differences. The siQuant assay results (Fig. 3A) showed that both modified siRNAs (RNA1, RNA2) improved their activities with statistical

Table 2 Sequences of D-isoNA modified siRNAs

| | No. | Name | Sequence |
|----------------------|-----|----------|---|
| Unmodified-1 | 30 | RNA1 | 1S/5'-AGAAUUGGUAUCUGGAUCAUtt-3' (1S/1A) 1A/5'-AUGAUCCAGAUCCAAUUCUtt-3' |
| Antisense modified-1 | 31 | 1S/1A08D | 1S/5'-AUGAUCC _{A_D} GAUCCAAUUCUtt-3' |
| Unmodified-2 | 32 | RNA2 | 2S/5'-AGCAUGAACCAUGAGUUGCtt-3' (2S/2A) 2A/5'-GCAACUCAUGGUUCAUGCUtt-3' |
| Antisense modified-2 | 33 | 2S/2A08D | 2S/5'-GCAACU _{C_{A_D}} UGGUUCAUGCUtt-3' |

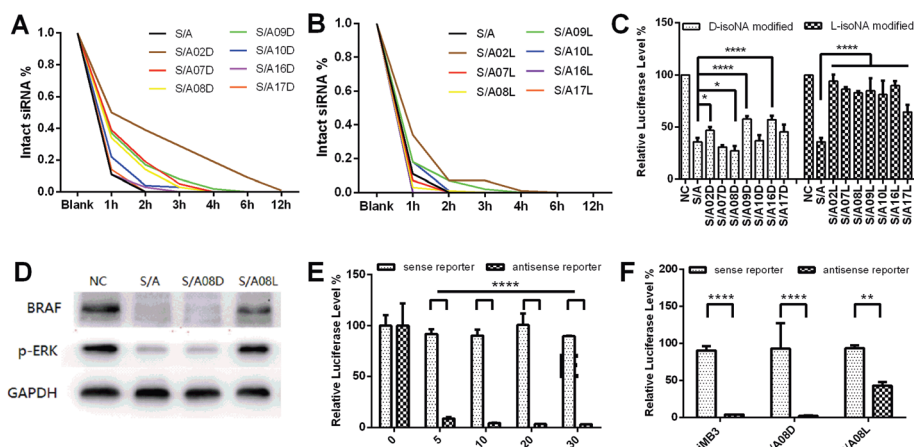


Fig. 2 Serum stability of siMB3s modified with D-isoNA (A) and L-isoNA (B) at the antisense strand. These siRNAs were incubated in 50% fetal bovine serum at 37 °C and sampled at various time points. Natural siRNA without serum treatment was the control sample to mark the intact siRNA band. (C) Firefly luciferase gene silencing activity of siMB3s modified with D-/L-isoNAs at the antisense strand (0.3 nM). (D) Western blot assay of BRAF and p-ERK proteins (2.0 nM). A375 cells were harvested for proteins 48 h post transfection. (E) Firefly luciferase gene silencing activity of the sense and antisense strands of siMB3. (F) Firefly luciferase gene silencing activity of siMB3 modified with D-/L-isoNAs at the 8th position (10 nM). (C, E, F) The relative luciferase level was normalized to the ratio of firefly luciferase and *Renilla* luciferase. Normalized expression in mock-transfected cells was treated as 100%.

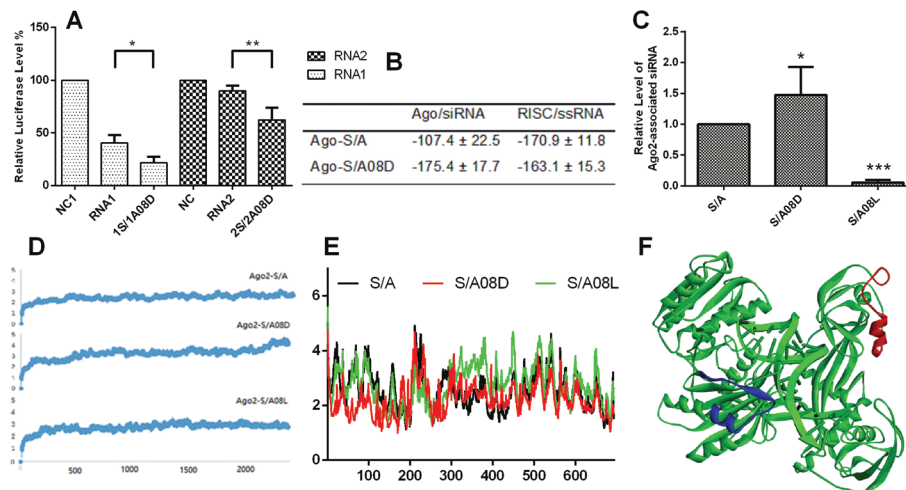


Fig. 3 (A) Firefly luciferase gene silencing activity of siRNAs modified with D -isoNAs at the 8th position (6 nM). The relative luciferase level was normalized to the ratio of *firefly* luciferase and *Renilla* luciferase. Normalized expression in mock-transfected cells was treated as 100%. (B) The binding free energies of Ago/siRNA and RISC/ssRNA for each of the models (kcal mol^{-1}). (C) Quantitative analysis of Ago2-associated siRNA. The Ago2 protein was obtained by immunoprecipitation 48 h post transfection, and the Ago2-associated antisense strand was extracted and quantified by real-time PCR. Unmodified siRNA in mock-transfected cells was treated as 100%. (D) RMSD of the complex of TtAgo and modified siRNA for 30 ns. The complex achieved equilibrium at 5–10 ns. (E) RMSF of each residue in the complex of TtAgo and modified siRNA at the 20 ns point. There were two peaks around the 220th and 495th residues in the natural and D -isoNA modified siRNA models, respectively. (F) The complex of TtAgo and the natural siRNA model. The red loop refers to the first RMSF peak representing the 210th–230th residues, and the blue loop refers to the second RMSF peak representing the 480th–510th residues as indicated.

significance, which indicated that activity enhancement of the siRNAs by modification with D -isoNA at the 8th position might be universal. The binding free energies (Fig. 3B) showed that the D -isoNA modified siMB3 bound earlier to Ago due to the lower free energy of Ago/siRNA. Moreover, the RISC/ssRNA complexes were destabilized with a higher free energy, which accelerated the sense strand separation.

RNA-binding protein immunoprecipitation (RIP) was evaluated to investigate the relationship between modification and the complex amount. The results showed that the 8th position modified with D -isoNA had a strong affinity to the Ago2 protein and a significant drop in the L -isoNA modification was detected (Fig. 3C). This was well consistent with the silencing activities.

Molecular dynamic simulation showed that the complex consisting of D -/ L -isoNA modified siRNAs and the Ago protein rapidly achieved equilibrium (Fig. 3D), and the RMSF of the simulated modes showed that there were two flexible loops in the Ago-S/A mode belonging to the PAZ and PIWI domains (Fig. 3E and F). The D -isoNA modified mode (Ago-S/A08D) was similar to the natural mode except that the PIWI domain was more stable. However, the L -isoNA modification (Ago-S/A08L) remarkably altered the steady state of the complex, which might influence the modified siRNAs binding to the Ago protein.

Sense strand of siRNAs modified with D -/ L -isoNAs

The degradation assays (Fig. 4A) and siQuant assays (Fig. 4B) of siRNAs modified with D -/ L -isoNAs on the sense strand were carried out as before. It was found that D -isoNA incorporation

in the sense strand had no obvious effects on the stability and silencing activity. However, the middle of the chain modified with L -isoNA (S10-13L/A) was able to improve the gene-silencing ability, even though these siRNAs were unstable in serum.

Both L -isoNA and mismatched pairs introduced into siRNAs lowered the T_m value, which activated RISC and enhanced activity. We further synthesized a series of mismatched siRNAs whose false priming sites were complementary to the 7th and 8th positions of the antisense strand (Table S2[†]), and their activity and thermodynamic stability were examined by the siQuant assays and melting temperature analysis (T_m) (Fig. 4C). The results showed that the modified position rather than the T_m reduction might play a role in the activity. In addition, gene-silencing had no marked variation at the 12th position even when the T_m value was reduced from 70.4 °C (S/A) to 64.0 °C (S13a/A). Nevertheless, the activity of the 13th position modified with L -isoNA (67.7 °C, S13L/A) exhibited a significant enhancement compared with the mismatched siRNAs (63.9 °C, S12c/A) despite its higher T_m value.

3'-Overhangs of siRNAs modified with D -/ L -isoNAs

3'-Overhangs of siRNAs modified with chemical molecules improved the biological properties. Incorporation of isoNAs into 3'-overhangs might affect the characteristics of siRNAs to varying degrees. First, we introduced double D -isoNA (base = uracil, D -isoU) into the siRNAs' 3'-overhangs in each strand (S/ADD, SDD/A). It was found that the 3'-overhang of the sense strand modification (SDD/A) significantly enhanced serum stability, while the antisense strand modification (S/ADD), as

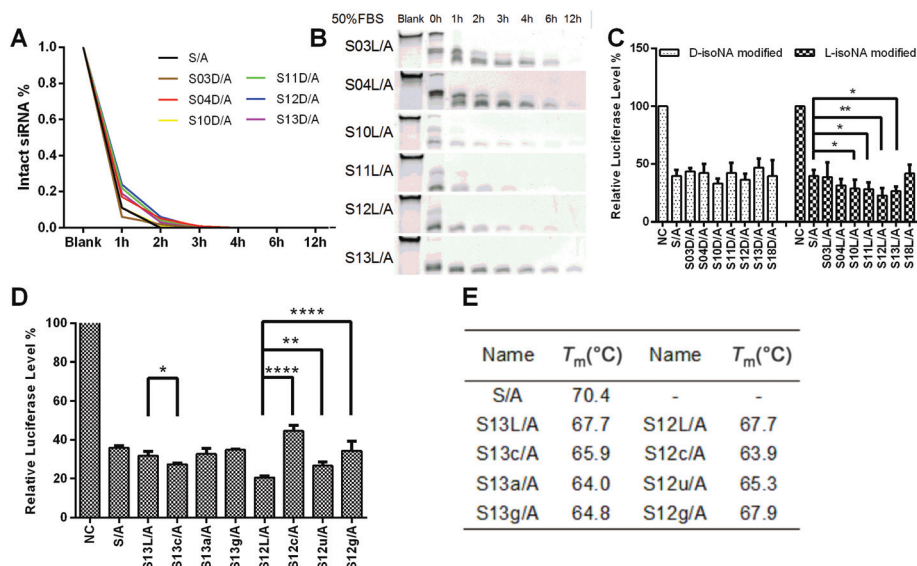


Fig. 4 Serum stability of siMB3s modified with D -isoNA (A) and L -isoNA (B) on the sense strand. These siRNAs were incubated in 50% fetal bovine serum at 37 °C and sampled at various time points. Natural siRNA without serum treatment was the control sample to mark the intact siRNA band. (C) Firefly luciferase gene silencing activity of siMB3s modified with D -/ L -isoNAs on the antisense strand (0.3 nM). (D) Firefly luciferase gene silencing activity of mismatched siRNAs. (C, D) The relative luciferase level was normalized to the ratio of the *firefly* luciferase and *Renilla* luciferase. Normalized expression in mock-transfected cells was treated as 100%. Data were from three replicates. (E) Thermal denaturation studies of L -isoNAs or mismatch incorporation in siRNAs.

well as a uracil mutation (Suu/A), had no prominent effects on the stability (Fig. 5A and S2†). Further study showed that a single D -isoU modification did not have much influence on the serum stability regardless of its position in the 3'-overhangs (SD/A, SDt/A, StD/A); however, two or three isoNA modifications strongly enhanced serum stability (Fig. 5B and S3†), and the stability of SDD/A exhibited statistical significance in comparison with other modifications (Fig. S4†), such as the 2'- O -MOE modification (Fig. 5C and S5†). Thus, the D -isoNA

modifications had unique superiority for use in the application of existing RNAi-based therapeutics (Table 3).

The ribonuclease degradation assay proved that the SDD/A sequence possessed strong exo-/endo-nuclease resistance (Fig. 5D and E), which explains its physiological and intracellular stability. Quantitative PCR analysis showed that SDD/A enhanced the duration of RNAi activity, and exhibited preferable silencing activity within 72 h. Thus, double D -isoUs incorporation into the 3'-overhangs of the sense strand might be an

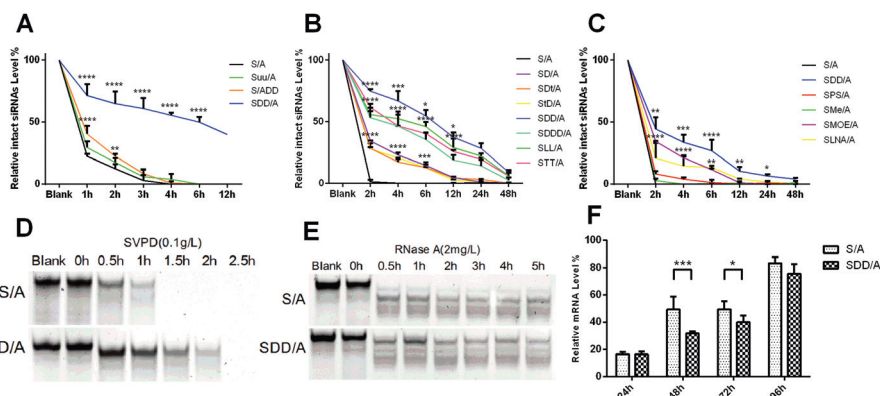


Fig. 5 (A–C) Serum stability of modified siRNAs. These siRNAs were incubated in 50%, 80%, and 90% fetal bovine serum at 37 °C. Intact siRNA was quantified by using Image Lab software, and the relative siRNA level was calculated with the percentage of the initial amount treated as 100%. The P -values of S/ADD, SD/A, and SMOE/A are compared with S/A, and the P -values of SDD/A are compared with S/ADD, SD/A, SMOE/A in the three figures, respectively. The data are from two replicates. (D) SVDP (0.1 g L⁻¹) cleavage assay of natural and modified siRNAs. (E) RNase A (2 mg L⁻¹) cleavage assay of natural and modified siRNAs. (D, E) These siRNAs were incubated at 37 °C and sampled at various time points, followed by separation on a 20% PAGE gel with siRNA products visualized by SYBR Gold staining. (F) Quantitative PCR analysis of Braf-mu mRNA (2 nM). Data are from three replicates.

Table 3 Sequences of chemically modified siMB3s at 3'-overhangs

| | No. | Name | Sequence |
|--|--|--------|---|
| Unmodified | 34 | Suu/A | 5'-GCUACAGAGAAAUCUCGAUUU-3'/A |
| Sense strand modification (matched with siMB3-As) | 35 | SDD/A | 5'-GCUACAGAGAAAUCUCGAU <i>U_DU_D</i> -3'/A |
| | 36 | SDDD/A | 5'-GCUACAGAGAAAUCUCGAU <i>U_DU_DU_D</i> -3'/A |
| | 37 | ST/A | 5'-GCUACAGAGAAAUCUCGAU <i>U_Dt</i> -3'/A |
| | 38 | StD/A | 5'-GCUACAGAGAAAUCUCGAU <i>tU_D</i> -3'/A |
| | 39 | SD/A | 5'-GCUACAGAGAAAUCUCGAU <i>U_D</i> -3'/A |
| | 40 | STT/A | 5'-GCUACAGAGAAAUCUCGAU <i>T_D</i> -3'/A |
| | 41 | SLL/A | 5'-GCUACAGAGAAAUCUCGAU <i>U_LU_L</i> -3'/A |
| | 42 | SpS/A | 5'-GCUACAGAGAAAUCUCGAU <i>t_s</i> -3'/A |
| | 43 | SMe/A | 5'-GCUACAGAGAAAUCUCGAU <i>U_{Me}U_{Me}</i> -3'/A |
| | 44 | SMOE/A | 5'-GCUACAGAGAAAUCUCGAU <i>T_{MOE}T_{MOE}</i> -3'/A |
| | 45 | SLNA/A | 5'-GCUACAGAGAAAUCUCGAU <i>T_{LNA}T_{LNA}</i> -3'/A |
| | Antisense strand modification (matched with siMB3-SS) | 46 | S/ADD |

The positions of the other nucleotides' incorporation are indicated in blue italic and bold. "B_{Me}" represents the 2'-O-methyl modification, "B_{MOE}" represents the 2'-O-methoxyethyl modification, "B_{LNA}" represents the locked nucleotide modification, "s" represents the phosphothioate modification.

effective chemical strategy for improving the stability and silencing-activity of siRNA.

Discussion

The process of the siRNA-induced RNAi approach is complex. siRNA first binds to a set of bioactive proteins to form the RISC loading complex (RLC).²⁶ Subsequently, the duplex is wound and the sense strand is cleaved and separated to form an active-RISC. The active-RISC facilitates binding to target mRNA and exhibits gene-silencing activity. Chemical modifications enable the improvement of biological properties by regulating parts of the RNAi process, and the ribonuclease resistance.²⁷ In addition, the incorporation of chemical molecules into different positions in siRNAs may lead to diverse characteristic variations.

The antisense strand of siRNA plays a vital role in its silencing activity. The chain directly interacts with the Ago2 protein and forms a significant component of active-RISC. All siRNAs modified with L-isoNA at the antisense strand exhibited a remarkable loss of silencing activity due to strong interference of siRNA binding to the Ago protein (shown in the S/A08L model). The L-isoNA modifications led to a significant conformational distortion, which led to the Ago protein being unable to bind to modified siRNA. However, the D-isoNA incorporated into the 2nd position of the antisense strand (S/A02D) significantly enhanced serum stability with a slight activity concession. It is possible that the position is proximal to the unstable thermodynamic terminus of the siRNA, where the regions were selected for directional invasion of the nuclease in serum.²⁸ In addition, only the 8th position of the antisense strand modified with D-isoNA exhibited a clear activity enhancement, which was observed in three individual siRNAs (S/A, RNA1, and RNA2). The Ago/siRNA complex of the S/A08D

model was stabilized with a lower free energy, which indicated that the modified siRNA was easily loaded into the RISC; however, the RISC/ssRNA complex was destabilized with a higher free energy, which accelerated sense strand separation and activated the RISC.²⁹ The result of the quantitative analysis of the Ago2-associated siRNA was consistent with the results of the molecular dynamics simulation. It represents that single D-isoNA modification was likely to adjust the conformation for meeting the requirement of interactional regions. It will help us understand the spatial structure of the acting sites. Additional studies showed that the siMB3 sequence exhibited excellent strand selection due to its observable thermodynamic differences, and the D/L-isoNA modification did not change the target specificity. Furthermore, D-isoNA incorporated into either the 9th or the 16th position reduced the level of gene-expression, which suggests these sites are conserved.

The sense strand of siRNA is usually tolerant of chemical modifications. It was found that the D-isoNAs incorporated into the sense strand (except for the 3'-overhangs) did not exhibit visible effects on their biological properties, including serum stability and silencing activity. The modified siRNAs showed no statistical significance in comparison with the unmodified siRNA. It is possible that chemical molecules are not directly involved in the RNAi approach, which is not enough to cause character variation. However, L-isoNA incorporation greatly impaired the serum stability to a large enough degree so that siRNAs immediately disappeared when mixed with fresh FBS. We believe that the modification led to an incompact conformation, which added a new vulnerable region for ribonuclease recognition. Furthermore, L-isoNA incorporated into the middle of the sense strand (S10-13L/A) slightly enhanced its silencing activity. siRNAs with the L-isoNA modification and a mismatch at the same position failed to verify whether the *T_m* value was primarily responsible for the silen-

cing enhancement. Certain mismatched siRNAs reduced the silencing activity, even though they showed a lower T_m value, and the activity change was not consistent with the T_m reduction. Therefore, the activity enhancement caused by L-isoNA incorporation into the middle of the sense strand cannot contribute to the decreasing thermodynamic stability.

The 3'-overhangs of siRNAs modified with chemical molecules improved their biological properties. Incorporation of the 3'-overhangs from the sense strand (but not the antisense strand) enhanced serum stability, which was consistent with previous reports, even though the PS was replaced by D-isoNAs. In addition, the SDD/A sequence exhibited the best stability of all of the chemical modifications, and had a unique superiority that could be used in the application of existing RNAi-based therapeutics. Extending the length of the 3'-overhangs did not enhance the serum stability any further. This indicates that double D-isoNAs achieved ideal protection of the siRNA from ribonuclease degradation, which was confirmed by exo-/endo-nuclease cleavage assays. Moreover, the activity evaluation showed that the SDD/A sequence prolonged the retention time in comparison with the unmodified siRNA. Thus, double D-isoU incorporation in the 3'-overhangs of the sense strand might be an effective chemical strategy for improving the stability and silencing-activity of siRNA.

Experimental

Synthesis and purification of RNA oligonucleotides

Synthesis of the RNA oligonucleotides was performed on a 394 DNA Synthesizer (Applied Biosystems, USA) at the 1 μmol scale according to standard phosphoramidite chemistry. D-isoNA and L-isoNA phosphoramidite monomers were synthesized according to our previous reports.³⁰ The coupling time used for natural RNA phosphoramidites with 2'-OTBDMS protected (A^{Bz} , C^{Ac} , G^{ibu} and U) was the standard 600 seconds, differing from that of D-/L-isoNA phosphoramidites, whose coupling time was extended to 900 seconds because of their steric effect. Deprotection and cleavage of the oligomers from the solid-phase support CPG were carried out in methylamine/methanol (1:1, v/v) at 60 °C for 1.5 h and desilylation was accomplished by treatment with Bu_4NF . The crude product was precipitated with 3 M sodium acetate followed by the addition of cold butanol and ethanol, and was subsequently purified by high-performance liquid chromatography using a base ion-exchange column (DionexDNAPac, PA200, 9 \times 250 mm). Phase B was 0.02 M Tris- HClO_4 with 10% ACN (pH 8.0), and phase A had extra 0.4 M NaClO_4 in eluent B. The purified oligonucleotides were then desalted by using a Sephadex G25 column (Fig. S6[†]), lyophilized to dryness for storage, and confirmed by MALDI-TOF MS and ESI MS analyses (Fig. S7[†]).

Serum siRNA degradation assays

siRNAs (1 μL , 20 μM) were incubated in PBS (10 μL) at 37 °C containing 50% FBS (Sigma-Aldrich Corp., St Louis, MO, USA).

The solution was removed after the indicated points of time and frozen in liquid nitrogen immediately. Following the addition of 6 \times RNA loading buffer (2 μL , DingGuo, Beijing, China), aliquots were analyzed on 20% polyacrylamide gels at 110 CV for 120 min and stained with 0.1% SYBR Gold to be visualized.

Ribonuclease cleavage assays

siRNAs (1 μL , 2 μM) were incubated with RNase A (2 mg L^{-1} , Sigma-Aldrich Corp., St Louis, MO, USA) or SVPDE (0.1 g L^{-1} , Sigma-Aldrich Corp., St Louis, MO, USA) at 37 °C in water. The solution was removed after the indicated time points, mixed with a ribonuclease inhibitor (1 μL) for 2 minutes, and frozen in liquid nitrogen. Following the addition of 6 \times RNA loading buffer (2 μL), the aliquots were analyzed on 20% polyacrylamide gels at 110 CV for 120 min and stained with 0.1% SYBR Gold to be visualized.

Cell culture and dual-luciferase assay

Human embryonic kidney 293 (HEK293) cells were grown in Dulbecco's modified Eagle's medium (DMEM, Macgene) supplemented with 10% fetal bovine serum (FBS, Corning), 100 U ml^{-1} penicillin, and 100 $\mu\text{g ml}^{-1}$ streptomycin (Macgene) at 37 °C in a 5% CO_2 humidified incubator.

Cells were seeded into 24-well plates at 5×10^4 cells per well 1 day before transfection. The siQuant vector (0.1 μg per well) carrying the target site of the tested siRNA and pRL-TK control vector (0.01 μg per well) was transfected into HEK293 cells by Lipofectamine 2000 (Invitrogen, USA), both with and without the siRNA (0.3 nM). After a 4 h incubation, 1.0 mL of the DMEM culture containing 10% FBS was added into the transfection medium. Cells were harvested 24 h after transfection and lysed with passive cell lysis. Dual luciferase activities were determined with 30 μL of the cell lysate using the Dual-Luciferase Assay System (Promega) by NOVOSTAR (BMG Lab Technologies GmbH, Germany). The silencing efficacy of each siRNA was calculated for comparison to a sample without siRNA treatment. All experiments were performed in triplicate.

Real-time PCR

Cells were seeded in 6-well plates at 2×10^5 cells per well 1 day before transfection. After the cells reached approximately 50% confluence, they were transfected with siRNAs encapsulated in Lipofectamine RNAiMAX (Invitrogen, USA) according to the manufacturer's protocols.

After the siRNAs were transfected for 48 h, RNA was extracted from the cells using the Trizol reagent (Life Technologies, USA) according to the standard chloroform extraction protocol. For cDNA synthesis, 1 μg of total RNA was reverse transcribed using the Reverse Transcription System (Promega, USA), according to the manufacturer's protocols. Then real-time PCR was performed using an Mx3005P real-time PCR System (Agilent Technologies, USA) and an SYBR Green qPCR Master Mix (Promega, USA). The primers used in the study were as follows: β -actin (forward, CCA ACC GCG AGA TGA; reverse, CCA GAG GCG TAC AGG GAT AG), and MB3 (forward, TGG

TGT GAG GGC TCC AGC TTGT; reverse, ATG GGA CCC ACT CCA TCG AGA TTT CT). PCR followed a three-step amplification protocol followed by a melting curve segment. The expression level was analyzed by the Ct (cycle threshold) values using a standard protocol.³¹

Western blot

Melanoma A375 cells were seeded into 6-well plates at 2×10^5 cells per well, 1 day before transfection. When the cells reached approximately 50% confluence, the siRNAs (2 nM) were transfected with Lipofectamine RNAiMAX (Invitrogen). The cells were collected and lysed 48 h after transfection. The protein concentration was measured by using a Flex Station 3 Benchtop Multi-Mode Microplate Reader (Molecular Devices, California, USA) at 562 nm. Proteins were separated on 30% Bis-Tris-polyacrylamide gels and then transferred to PVDF membranes (Millipore, Bedford, USA). After blocking with 5% skim milk overnight, the membranes were probed with primary antibodies against GAPDH (1:4000, Cell Signaling Technology, MA, USA), B-RAF (1:2000, Abcam, MA, USA), or p-ERK (1:4000, Cell Signaling Technology, MA, USA) at 4 °C overnight and then incubated with a secondary antibody (1:4000, Santa Cruz Biotechnology, Santa Cruz, USA) in 5% skim milk for 3 h. Proteins were analyzed by using Image Lab™ software (ChemiDoc™ XRS System, BIO-RAD, CA, USA) and normalized against the GAPDH protein expression levels.

Thermal denaturation studies (T_m)

The hyperchromicity curves of the hybridized duplex solution $1 \mu \text{ min}^{-1}$ T_m buffer (5.7 mM Tris-HCl, pH 7.5, 5.7 mM KCl, 0.1 mM MgCl₂) were recorded on a Varian Cary 300 Bio UV-visible spectrophotometer. The absorbance was recorded in the reverse and forward directions at a temperature range of 25–90 °C at a rate of 0.3 °C min⁻¹ at the settled wavelength of 260 nm.

RNA-binding protein immunoprecipitation assay (RIP)

The cells were lysed at 48 h post transfection in lysis buffer (Beyotime Institute of Biotechnology, Suzhou, China). The Ago2 antibody (Cell Signaling Technology, MA, USA) was incubated with magnetic protein G dynabeads (Life Technologies AS, Oslo, Norway) at 4 °C for 2 h on a rotator. After washing twice with washing buffer to remove unbound antibodies, the beads were added to the cell lysis above and rotated at 4 °C overnight. Ago2, as well as the containing siRNAs, were eluted from the beads by an eluent (Life Technologies AS, Oslo, Norway) and then neutralized immediately with an equal volume of 1 M Tris-HCl (pH = 8.0). Twenty U of proteinase K was used to hydrolyze the Ago2 at 65 °C for 10 min and the siRNAs were quantified by stem-loop RT-PCR.

Stem-loop RT-PCR for siRNA detection was performed using TaqMan miRNA assays followed by SYBR Green based real-time PCR. Five microliters of the eluent and the stem-loop RT primer (50 nM, synthesized by Ribobio, Guangzhou, China) were denatured at 85 °C for 5 minutes, and then at 60 °C for 5 minutes. cDNA was synthesized by using the

TaqMan MicroRNA Reverse Transcription Kit (Applied Biosystems, USA). The reverse transcription reaction was incubated at 16 °C for 30 minutes, 42 °C for 30 minutes, and 85 °C for 5 minutes, and then stored at 4 °C. Real-time PCR was performed in 20 μL of the PCR reaction mixture including 1.5 μL of the RT product, 1 \times GoTaq qPCR Master Mix (Promega, USA), and 0.5 μM of the forward primer and reverse primer. The reaction was incubated at 95 °C for 10 min, followed by 40 cycles of 95 °C for 15 seconds and 60 °C for 1 min. The content of the siRNA was measured by relative quantification and u6 snoRNA was used as an internal reference.

Molecular structures of the Ago/siRNA complex

The crystal structures of the Ago2 protein without the siRNA duplex have been reported.³² The *T. thermophilus* Ago protein could be used as a substitute due to the Ago family sharing a high structural similarity. The crystal structure termed 3HVR was chosen as the subject for its complete structure. The two-stranded siRNA duplex came from 3HK2, and the original nucleotides were substituted in the siMB3 sequence. An iso-nucleotide was incorporated into a set position, and molecular simulation was carried out to obtain the complex composed of the D-/L-isoNA modified siRNA and Ago protein through Discovery Studio 2.5 software according to an exemplary method.^{18b} A scale of the abscissa represented the serial number of the residues in the complex.

Molecular dynamics simulation

All of the dynamics simulations were performed in Amber 11. The complex was parceled in an octahedral water box, and the minimum distance between them was 10 Å. The SHAKE algorithm was applied to restrain the hydrogen atoms, as the TIP3P water model, as well as sodium ions, was used to neutralize the system. In addition, the electrostatic interaction was evaluated utilizing the particle mesh Ewald (PME) principle. The integration time step was set to 1 fs and the results were automatically saved every 10 ps. The Ago-siRNA complex was restricted by the steepest descent for 5000 steps and the conjugate gradient pathways in the case of water molecules' contact, and minimization of the systems was performed in the same way. Then, the general heating equilibrium-production pipeline was carried out in the separated minimized systems. First, the systems underwent heating under the NVT ensemble mode from 0 K to 300 K in 20 ps with a 10 kcal mol⁻¹ Å⁻² harmonic constraint. Second, the systems underwent an equilibrium process under the NPT ensemble mode, with the harmonic constraint reduced to 0. Finally, the last 10–20 ns trajectory production was applied to the analysis. The scale of the abscissa represented the serial number of residues in the complex.

MM/PBSA binding free energy calculation

The binding free energy was calculated by using the equation: $\Delta G_{b,s} = \Delta G_{b,v} + \Delta G_{s,c} - (\Delta G_{s,l} + \Delta G_{s,r})$, where $\Delta G_{b,s}$ and $\Delta G_{b,v}$ are the binding free energies in the solution and in a vacuum, respectively. $\Delta G_{s,c}$, $\Delta G_{s,l}$ and $\Delta G_{s,r}$ represent the free energies

of the complex, ligand and receptor, respectively. $\Delta G_{b,v}$ is composed of the interaction energy as well as the entropy contribution between the ligand and the receptor. Solvation free energy contained both a hydrophobic part and an electrostatic part. In this case, the binding free energies for the complexes of Ago/siRNA and RISC/ssRNA were calculated with the MM/PBSA pathway excluding the entropy contribution through AmberTools 1.5. software with the MMPBSA.py module.

Statistical analysis

One-way repeated measures analysis of variance (ANOVA) was used for the analysis of the experimental data. All data are average experimental values, and error bars denoted standard deviations. As appropriate, the significant differences were represented by *P*-values obtained with Student's *t*-test: **P* < 0.05; ***P* < 0.01; ****P* < 0.001; or *****P* < 0.0001. All statistical analyses were carried out using GraphPad Prism 6.0 software.

Conclusion

D-/L-isoNAs were incorporated into different positions of the siRNA duplex, leading to an enhancement of nuclease resistance as well as an improvement in gene-silencing abilities. The activity tended to be site-specific when D-isoNA was incorporated into the antisense strand of the siMB3 duplex. When the siRNA sequence was modified at the 8th position with a single D-isoNA analog, the silencing activity improved, which was assessed by a western blot, molecular dynamics simulation, and stem-loop RT-PCR. These data suggest that D-isoNA modified the 8th position of the antisense strand and enhanced the loading of the siRNA into Ago2, promoting hydrolysis of the sense strand to form an active RISC. In addition, the D-isoNA modification was well tolerated in the RNAi machinery at the sense strand, particularly for the 3'-overhangs. Double D-isoNA modifications can enhance exo-/endo-nuclease resistance, and prolong the silencing retention time. However, L-isoNA incorporated into the antisense strand significantly reduced the silencing activity. These modifications had evident effects on the siRNA interaction with the Ago2 protein, and remarkably decreased the level of the guide strand associated with the RISC; however, L-isoNA incorporated into the center (the 10th–13th positions) of the sense strand slightly enhanced silencing. Thus, D-/L-isoNA can be applied as a useful tool to examine the conformational requirement between nucleic acids and the Ago2 protein, and improve siRNA efficacy.

Conflict of interest statement

None declared.

Acknowledgements

This work was supported by the Ministry of Science and Technology of China [2012AA022501, 2012CB720604] and the

National Natural Science Foundation of China [20932001]. Funding for open access charge: Ministry of Science and Technology.

Notes and references

- 1 A. Fire, S. Xu, M. K. Montgomery, S. A. Kostas, S. E. Driver and C. C. Mello, *Nature*, 1998, **391**, 806–811.
- 2 S. M. Elbashir, J. Harborth, W. Lendeckel, A. Yalcin, K. Weber and T. Tuschl, *Nature*, 2001, **411**, 494–498.
- 3 B. L. Davidson and P. B. McCray Jr., *Nat. Rev. Genet.*, 2011, **12**, 329–340.
- 4 J. J. Turner, S. W. Jones, S. A. Moschos, M. A. Lindsay and M. J. Gait, *Mol. Biosyst.*, 2007, **3**, 43–50.
- 5 M. Robbins, A. Judge and I. MacLachlan, *Oligonucleotides*, 2009, **19**, 89–102.
- 6 A. L. Jackson and P. S. Linsley, *Nat. Rev. Drug Discovery*, 2010, **9**, 57–67.
- 7 (a) S. Choung, Y. J. Kim, S. Kim, H. O. Park and Y. C. Choi, *Biochem. Biophys. Res. Commun.*, 2006, **342**, 919–927; (b) M. A. Behlke, *Oligonucleotides*, 2008, **18**, 305–319.
- 8 J. B. Bramsen, M. B. Laursen, A. F. Nielsen, T. B. Hansen, C. Bus, N. Langkjaer, B. R. Babu, T. Hojland, M. Abramov, A. Van Aerschot, D. Odadzic, R. Smicius, J. Haas, C. Andree, J. Barman, M. Wenska, P. Srivastava, C. Zhou, D. Honcharenko, S. Hess, E. Muller, G. V. Bobkov, S. N. Mikhailov, E. Fava, T. F. Meyer, J. Chattopadhyaya, M. Zerial, J. W. Engels, P. Herdewijn, J. Wengel and J. Kjems, *Nucleic Acids Res.*, 2009, **37**, 2867–2881.
- 9 Y. Huang, Z. Chen, Z. Wang, Y. T. Li, Y. Chen, Z. J. Yang and L. H. Zhang, *Sci. China: Chem.*, 2014, **57**, 329–334.
- 10 J. S. Parker, S. M. Roe and D. Barford, *Nature*, 2005, **434**, 663–666.
- 11 M. H. Jo, S. Shin, S. R. Jung, E. Kim, J. J. Song and S. Hohng, *Mol. Cell*, 2015, **59**, 117–124.
- 12 N. T. Schirle, G. A. Kinberger, H. F. Murray, W. F. Lima, T. P. Prakash and I. J. MacRae, *J. Am. Chem. Soc.*, 2016, **138**, 8694–8697.
- 13 (a) T. P. Prakash, C. R. Allerson, P. Dande, T. A. Vickers, N. Sioufi, R. Jarres, B. F. Baker, E. E. Swayze, R. H. Griffey and B. Bhat, *J. Med. Chem.*, 2005, **48**, 4247–4253; (b) J. Zheng, L. Zhang, J. Zhang, X. Wang, K. Ye, Z. Xi, Q. Du and Z. Liang, *FASEB J.*, 2013, **27**, 4017–4026; (c) A. Kannan, E. Fostvedt, P. A. Beal and C. J. Burrows, *J. Am. Chem. Soc.*, 2011, **133**, 6343–6351.
- 14 N. T. Schirle, J. Sheu-Gruttadauria and I. J. MacRae, *Science*, 2014, **346**, 608–613.
- 15 A. Lingel, B. Simon, E. Izaurralde and M. Sattler, *Nat. Struct. Mol. Biol.*, 2004, **11**, 576–577.
- 16 Y. Wang, S. Juranek, H. Li, G. Sheng, G. S. Wardle, T. Tuschl and D. J. Patel, *Nature*, 2009, **461**, 754–761.
- 17 (a) S. L. Ameres, J. Martinez and R. Schroeder, *Cell*, 2007, **130**, 101–112; (b) H. Tafer, S. L. Ameres, G. Obernosterer, C. A. Gebeshuber, R. Schroeder, J. Martinez and I. L. Hofacker, *Nat. Biotechnol.*, 2008, **26**, 578–583.

- 18 (a) H. W. Yu, L. R. Zhang, J. C. Zhou, L. T. Ma and L. H. Zhang, *Bioorg. Med. Chem.*, 1996, **4**, 609–614; (b) Y. Huang, Z. Chen, Y. Chen, H. Zhang, Y. Zhang, Y. Zhao, Z. Yang and L. Zhang, *Bioconjugate Chem.*, 2013, **24**, 951–959; (c) Z. Guan, H. W. Jin, Z. J. Yang, L. R. Zhang and L. H. Zhang, *Drug Discoveries Ther.*, 2007, **1**, 65–72.
- 19 Y. Huang, M. Tian, Y. Zhang, G. Sheng, Z. Chen, Y. Ma, Y. Chen, Y. Peng, Y. L. Zhao, Y. Wang, L. Zhang and Z. Yang, *Org. Biomol. Chem.*, 2015, **13**, 10825–10833.
- 20 P. Karki, X. Li, D. Schrama and L. Fliegel, *J. Biol. Chem.*, 2011, **286**, 13096–13105.
- 21 H. W. Lo, S. C. Hsu and M. C. Hung, *Breast Cancer Res. Treat.*, 2006, **95**, 211–218.
- 22 P. J. Roberts and C. J. Der, *Oncogene*, 2007, **26**, 3291–3310.
- 23 J. Haupenthal, C. Baehr, S. Kiermayer, S. Zeuzem and A. Piiper, *Biochem. Pharmacol.*, 2006, **71**, 702–710.
- 24 (a) J. Hong, Y. Huang, J. Li, F. Yi, J. Zheng, H. Huang, N. Wei, Y. Shan, M. An, H. Zhang, J. Ji, P. Zhang, Z. Xi, Q. Du and Z. Liang, *FASEB J.*, 2010, **24**, 4844–4855; (b) P. C. Patel, L. Hao, W. S. Yeung and C. A. Mirkin, *Mol. Pharm.*, 2011, **8**, 1285–1291.
- 25 F. Frank, N. Sonenberg and B. Nagar, *Nature*, 2010, **465**, 818–822.
- 26 H. W. Wang, C. Noland, B. Siridechadilok, D. W. Taylor, E. Ma, K. Felderer, J. A. Doudna and E. Nogales, *Nat. Struct. Mol. Biol.*, 2009, **16**, 1148–1153.
- 27 M. A. Behlke, *Oligonucleotides*, 2008, **18**, 305–319.
- 28 Y. Huang, Y. Ma, Y. Guo, L. Zou, H. Jin, L. Zhong, Y. Wu, L. Zhang and Z. Yang, *ChemMedChem*, 2014, **9**, 2111–2119.
- 29 G. B. Robb and T. M. Rana, *Mol. Cell*, 2007, **26**, 523–537.
- 30 (a) Z. J. Yang, H. Y. Zhang, J. M. Min, L. T. Ma and L. H. Zhang, *Helv. Chim. Acta*, 1999, **82**, 2037–2043; (b) J. Zhang, Y. Chen, Y. Huang, H. W. Jin, R. P. Qiao, L. Xing, L. R. Zhang, Z. J. Yang and L. H. Zhang, *Org. Biomol. Chem.*, 2012, **10**, 7566–7577.
- 31 T. D. Schmittgen and K. J. Livak, *Nat. Protoc.*, 2008, **3**(6), 1101–1108.
- 32 S. M. Elbashir, W. Lendeckel and T. Tuschl, *Genes Dev.*, 2001, **15**, 188–200.